

Probabilistic amplitude shaping for continuous-variable quantum key distribution with discrete modulation

Michele N. Notarnicola, Stefano Olivares, Enrico Forestieri, *Senior Member, IEEE*,
Luca Potì, *Senior Member, IEEE*, and Marco Secondini *Senior Member, IEEE*

Abstract

To achieve the maximum information transfer and face a possible eavesdropper, the samples transmitted in continuous-variable quantum key distribution (CV-QKD) protocols are to be drawn from a continuous Gaussian distribution. As a matter of fact, in practical implementations the transmitter has a finite (power) dynamics and the Gaussian sampling can be only approximated. This requires the quantum protocols to operate at small powers. In this paper, we show that a suitable probabilistic amplitude shaping of a finite set of symbols allows to approximate at will the optimal channel capacity also for increasing average powers. We investigate the feasibility of this approach in the framework of CV-QKD, propose a protocol employing discrete quadrature amplitude modulation assisted with probabilistic amplitude shaping, and we perform the complete security analysis in ideal conditions.

Index Terms

Continuous-variable quantum key distribution, probabilistic amplitude shaping.

I. INTRODUCTION

CURRENT cryptographic systems for communications security are mostly based on public-key cryptography, which allows two parties (Alice and Bob) to exchange confidential messages without pre-sharing a secret key—an important characteristic that makes this technique particularly suitable for many practical applications. Unfortunately, public-key cryptography offers only conditional security, as it usually relies on some assumptions about the computational resources of the eavesdropper (Eve) and the complexity of an underlying mathematical problem (e.g., the difficulty of factoring large integers in the Rivest-Shamir-Adleman (RSA) algorithm [1]).

On the other hand, the one-time pad [2] (or analogous cryptographic techniques) offer unconditional security (guaranteed by information theory) but with a much less practical implementation, as they require Alice and Bob to share in advance a secret key with the same length as the confidential message, to keep it secret, and to use it only once [3]. In practice, the one-time pad technique moves the security problem from the transmission of the confidential message to the distribution of a secure key. As distributing very long keys is not convenient and may pose a significant security risk, public-key cryptography is more widely used than the one-time pad.

A possible solution to the key distribution problem is offered by quantum key distribution (QKD) protocols [4]–[6], in which Alice and Bob share a secret key through the exchange of quantum states. The very laws of quantum mechanics guarantee the unconditional security of QKD protocols [7]; any measurement of the quantum states performed by Eve leaves a trace on the states themselves, allowing Alice and Bob to detect the intrusion, evaluate the amount of information possibly gained by Eve, and discard the key if necessary [8].

A promising approach to QKD is the one based on continuous variables (CVs) [6], [9]–[12]. With respect to discrete-variable (DV) protocols [4], in which single photons are typically used as information carriers, CV protocols use coherent states [13] (namely, laser pulses) to carry information, exactly as in classical communication systems. Unlike DV-QKD, CV-QKD does not require single-photon sources and detectors and can use the same devices and modulation/detection schemes commonly employed in classical coherent optical communications [14]–[16]. Therefore, we expect that the implementation of a CV-QKD system could also benefit from the use of the most effective modulation/detection techniques and digital processing strategies that have been developed for classical systems in the last years.

An important issue concerning CV-QKD is the modulation of coherent states. Although the first CV-QKD protocols were originally based on discrete modulations [9], [17], [18], in later protocols the states are modulated with a Gaussian distribution

Manuscript received November 11, 2022. This work has been partially supported by MAECI, Project No. PGR06314 “ENYGMA”, and by University of Milan, Project No. RV-PSR-SOE-2020-SOLIV “S-O PhoQuLis”. (*Corresponding author: Stefano Olivares*)

Michele N. Notarnicola and Stefano Olivares are with the Dipartimento di Fisica “Aldo Pontremoli”, Università degli Studi di Milano, I-20133 Milano, Italy, and also with INFN, Sezione di Milano, I-20133 Milano, Italy (e-mail: stefano.olivares@fisica.unimi.it).

Enrico Forestieri and Marco Secondini are with the TeCIP Institute, Scuola Superiore Sant’Anna, I-56124, Pisa, Italy, and also with National Laboratory of Photonic Networks, CNIT, I-56124 Pisa, Italy (e-mail: marco.secondini@santannapisa.it).

Luca Potì is with the National Laboratory of Photonic Networks, CNIT, I-56124 Pisa, Italy.

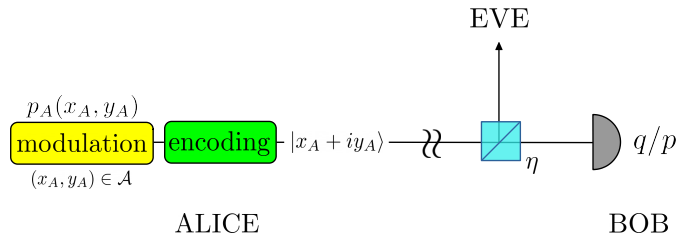


Figure 1. Schematic representation of the CV-QKD protocol discussed in the paper for a discrete modulation format. Alice generates symbols x_A and y_A , encodes them onto $|x_A + iy_A\rangle$ and sends them to Bob through a lossy quantum channel. Bob investigates the channel by performing a homodyne measurement of q/p , chosen at random.

[6], [10], [11]. This choice is related to the fundamental objective of maximizing the key generation rate (KGR), that is, the length of the secret key shared by Alice and Bob per unit time. Indeed, the actual KGR of a QKD system is limited by the difference between the amount of information that can be reliably transmitted from Alice to Bob per unit time and that obtainable by Eve. The maximization of the first quantity (which yields the channel capacity) is a classical problem in digital communications and is achieved with a Gaussian input distribution [19], [20].

Although justified on a theoretical level, Gaussian modulation involves several practical difficulties and is never used in classical digital communication systems for a twofold reason. The main drawback is that any realistic transmitter may generate signals up to a threshold power, whereas sampling a Gaussian distribution implies a nonzero probability of drawing a very large sample, and such a probability increases with the average channel power. Hence, a quantum communication system has to be operated at small powers. Furthermore, from the implementation point of view, the inevitable use of analog-to-digital converters, that have a finite number of bits at the transmitter, introduces a discretization of the sampling distribution. Thus, a more feasible way to perform quantum communication at higher average power without exceeding the transmitter dynamics is that of employing discrete modulation formats of appropriate order. This can be achieved by using a discrete probability distribution of the symbols that approximates the Gaussian one. In this way, by increasing the modulation order and by means of proper techniques one could approach at will the channel capacity for increasing average powers.

For instance, probabilistic amplitude shaping (PAS) is a practical coded modulation scheme that combines quadrature amplitude modulation (QAM), probabilistic constellation shaping, and forward error correction (FEC) to closely approach optimal channel capacity [21]–[23]. PAS uses a distribution matcher to map uniformly distributed information bits on QAM symbols with the desired target distribution [24]–[26]. In particular, a Maxwell–Boltzmann target distribution is considered, which maximizes the source entropy for a given discrete constellation and mean energy per symbol [27] (in practice, lower-energy symbols are used more often than higher-energy symbols, reducing the energy required to achieve a certain information rate). PAS can be easily combined with the efficient FEC codes and the corresponding decoding algorithms commonly employed in digital communications (e.g., binary LDPC codes with iterative belief propagation), obtaining an excellent trade-off between performance and complexity [22], [28], [29]. Ease of implementation, nearly optimal performance, fine rate tunability, and compatibility with existing devices and techniques make PAS one of the most popular solutions for the latest generation of coherent optical systems. These considerations suggest that a similar solution might be convenient also for CV-QKD. Indeed, there has been renewed interest in CV-QKD systems with discrete modulations [30]–[37].

In this work, we consider a CV-QKD protocol implemented through coherent states and homodyne detection [6], [9]–[12]. We start from the original proposal by Grosshans and Grangier (GG02) [6], and investigate its performance when the sender exploits discrete modulation (DM) assisted with PAS [21], [23] rather than continuous modulation (CM). In particular, we consider different QAM constellations [38], [39], optimize the shaping parameter and compare the performance of the original and modified protocols, with direct or reverse reconciliation, under individual or collective attacks.

The structure of the paper is the following. In Sec. II, we introduce the basic tools of CV-QKD and the results of the GG02 protocol. Then Sec. III presents our proposal of a CV-QKD scheme employing discrete modulation and based on standard probabilistic shaping, namely, optimizing the discrete probability distribution over the capacity of the channel. Instead, in Sec. IV we propose a new optimization procedure for PAS and discuss its performance. In Sec. V we close the paper by drawing some concluding remarks and their future developments.

II. BASICS OF CV-QKD

The most relevant protocol of CV-QKD is the so called GG02, proposed by Grosshans and Grangier in 2002 and employing continuous modulation (CM). It can be designed in two equivalent versions, the prepare-and-measure (PM) [6], [10] and the entanglement-based (EB) [11]. In this paper we will adopt the PM scheme. In GG02, Alice (A), the sender, encodes the information on several laser pulses described by coherent states $|x_A + iy_A\rangle$, where $x_A, y_A \in \mathbb{R}$ are randomly generated according

to a normal distribution \mathcal{N}_{Σ^2} , namely,

$$\mathcal{N}_{\Sigma^2}(z) = \frac{\exp[-z^2/(2\Sigma^2)]}{\sqrt{2\pi\Sigma^2}} \quad (z = x_A, y_A). \quad (1)$$

Therefore, the overall state generated by Alice is described by the density matrix

$$\begin{aligned} \rho_A &= \int_{\mathbb{R}^2} dx_A dy_A \mathcal{N}_{\Sigma^2}(x_A) \mathcal{N}_{\Sigma^2}(y_A) |x_A + iy_A\rangle \langle x_A + iy_A| \\ &= \nu^{\text{th}}(2\Sigma^2) \end{aligned} \quad (2)$$

that is a pseudo-thermal state

$$\nu^{\text{th}}(\bar{n}) = \frac{1}{\bar{n} + 1} \sum_{n=0}^{\infty} \left(\frac{\bar{n}}{\bar{n} + 1} \right)^n |n\rangle \langle n| \quad (3)$$

$\bar{n} = 2\Sigma^2$ being the mean energy, i.e. mean number of photons per symbol, and $|n\rangle$ representing the Fock state with n photons [13]. Accordingly, the modulation variance Σ^2 quantifies the average energy used for the encoding procedure.

The states are sent to the receiver, Bob (B), through an untrusted quantum channel which may be attacked by an eavesdropper, Eve (E). Bob probes the received signal by implementing the measurement of one of the two orthogonal quadratures q or p , $[q, p] = 2i\sigma_0^2$, where σ_0^2 represents the shot-noise variance, that is the vacuum fluctuations $\langle 0|q^2|0\rangle = \langle 0|p^2|0\rangle = \sigma_0^2$. The measured quadrature is chosen at random and implemented by performing homodyne detection [13]. Without loss of generality, to carry on the security analysis can assume that Bob measures q , obtaining the outcome x_B with probability $p_B(x_B)$. The amount of shared information corresponds to the mutual information [40]

$$I_{AB}^{(\text{CM})} = H_A + H_B - H_{AB} \quad (4)$$

where H_A , H_B , and H_{AB} are the Shannon entropies [40] associated with the probability distribution $p_A(x_A) = \mathcal{N}_{\Sigma^2}(x_A)$, $p_B(x_B)$ and the joint probability $p_{AB}(x_A, x_B) = p_A(x_A) p_{B|A}(x_B | x_A)$, respectively.

Straightforward calculations lead to

$$I_{AB}^{(\text{CM})} = \frac{1}{2} \log_2 [1 + \text{SNR}(\Sigma^2)] \quad (5)$$

where

$$\text{SNR}(\Sigma^2) = 4\eta\Sigma^2 \quad (6)$$

represents the signal-to-noise ratio at the receiver, which is proportional to the modulation variance Σ^2 and channel transmissivity η [6], [39]. Moreover, (5) coincides with the capacity of an additive white Gaussian noise (AWGN) channel as derived in the Shannon-Hartley theorem [19], [41], [42].

The second part of the protocol consists in the extraction of the secure key, where Alice and Bob share correlated classical information through a classical authenticated channel. This latter process is divided into three steps: channel evaluation [11], reconciliation [11], [43] and privacy amplification [11], [44]. Moreover, reconciliation can occur according to two alternatives: direct reconciliation (DR) if information is publicly shared by Alice or reverse reconciliation (RR) if it is Bob to publicly reveal what outcomes he retrieved [11]. For the sake of simplicity, we consider a perfectly efficient reconciliation process. Otherwise, in the presence of a reconciliation efficiency $\alpha < 1$ the mutual information is changed into $I_{AB} \rightarrow \alpha I_{AB}$ [32], [35].

If $\eta \leq 1$ represents the channel transmissivity, to assess the security of the channel we should assume that the lost signal is used by Eve to retrieve some information. Usually, one can represent this scenario as the presence on the channel, assumed to be lossless, of a beam splitter with transmissivity η : part of the signals are the reflected toward the eavesdropper (see Fig. 1). The attacks attempted by Eve are twofold: either individual attacks performed by measuring each single signal sent by Alice, or collective attacks. In the latter, Eve collects all the intercepted signals and performs a collective measurement on them only at the end of the reconciliation process [11]. In the case of individual attacks, the three involved parties share only classical information. Therefore, the KGR is obtained as the difference between the (classical) mutual information shared [6], namely

$$\begin{aligned} K_{\text{D,ind}}^{(\text{CM})} &= I_{AB}^{(\text{CM})} - I_{AE}^{(\text{CM})} \\ &= \frac{1}{2} \log_2 \left[\frac{1 + \eta\Sigma^2}{1 + (1 - \eta)\Sigma^2} \right] \quad (\text{with DR}) \end{aligned} \quad (7a)$$

$$\begin{aligned} K_{\text{R,ind}}^{(\text{CM})} &= I_{AB}^{(\text{CM})} - I_{BE}^{(\text{CM})} \\ &= \frac{1}{2} \log_2 \left[\frac{1 + \Sigma^2}{1 + (1 - \eta)\Sigma^2} \right] \quad (\text{with RR}) \end{aligned} \quad (7b)$$

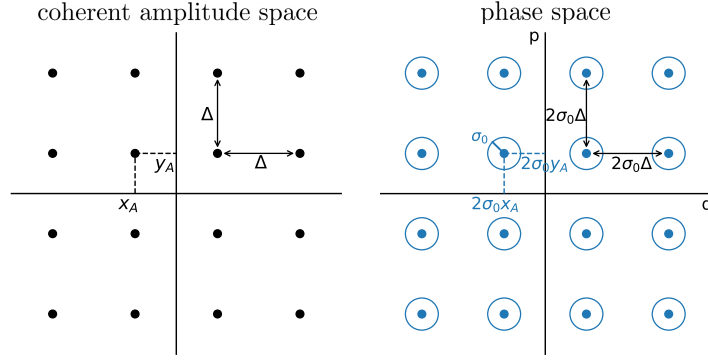


Figure 2. The constellation of pulses for the case $M = 4$ (QAM16), represented in both the complex space of coherent amplitudes and the (quantum) phase space.

where $I_{AE}^{(\text{CM})} = H_A + H_E - H_{AE}$ and $I_{BE}^{(\text{CM})} = H_B + H_E - H_{BE}$ in analogy to (4). In the first case, $K_{\text{D,ind}}^{(\text{CM})} > 0$ only if $\eta > 1/2$, due to the symmetry of the channel, while in the second case there is no threshold transmissivity and $K_{\text{R,ind}}^{(\text{CM})} > 0 \forall \eta$.

On the other hand, if Eve exploits a collective attack, the state of the whole sample is described by a statistical mixture $\rho_E = \int dx_A \mathcal{N}_{\Sigma^2}(x_A) \rho_{E|x_A}$ (in DR) or $\rho_E = \int dx_B p_B(x_B) \rho_{E|x_B}$ (in RR). Assuming Eve to implement the best possible collective measurement, we obtain the maximum mutual information she can achieve, namely the Holevo information [45]

$$\begin{aligned} \chi_{AE}^{(\text{CM})} &= S[\rho_E] - \int dx_A \mathcal{N}_{\Sigma^2}(x_A) S[\rho_{E|x_A}] \\ &= \log_2 \left(\frac{V_E + 1}{\sqrt{V_E + 1}} \right) + \frac{V_E - 1}{2} \log_2 \left(\frac{V_E + 1}{V_E - 1} \right) - \frac{\sqrt{V_E} - 1}{2} \log_2 \left(\frac{\sqrt{V_E} + 1}{\sqrt{V_E} - 1} \right) \end{aligned} \quad (8a)$$

$$\begin{aligned} \chi_{BE}^{(\text{CM})} &= S[\rho_E] - \int dx_B p_B(x_B) S[\rho_{E|x_B}] \\ &= \log_2 \left(\frac{V_E + 1}{\bar{V}_E + 1} \right) + \frac{V_E - 1}{2} \log_2 \left(\frac{V_E + 1}{V_E - 1} \right) - \frac{\bar{V}_E - 1}{2} \log_2 \left(\frac{\bar{V}_E + 1}{\bar{V}_E - 1} \right) \end{aligned} \quad (8b)$$

where

$$V_E = 1 + 4(1 - \eta)\Sigma^2 \quad (9a)$$

$$\bar{V}_E = \sqrt{\frac{\eta + (1 - \eta)(1 + 4\Sigma^2)}{1 - \eta + \eta(1 + 4\Sigma^2)}} (1 + 4\Sigma^2) \quad (9b)$$

and $S[\rho] = \text{Tr}(\rho \log_2 \rho)$ denotes the von Neumann entropy associated with the density matrix ρ [39]. The resulting KGR [46] reads

$$K_{\text{D, coll}}^{(\text{CM})} = I_{AB}^{(\text{CM})} - \chi_{AE}^{(\text{CM})} \quad (\text{with DR}) \quad (10a)$$

$$K_{\text{R, coll}}^{(\text{CM})} = I_{AB}^{(\text{CM})} - \chi_{BE}^{(\text{CM})} \quad (\text{with RR}) \quad (10b)$$

respectively. With respect to the individual attack case, now $K_{\text{D, coll}}^{(\text{CM})} > 0$ only if η is larger than a threshold transmissivity $\eta > \eta_{\text{th}}(\Sigma^2)$ larger than $1/2$ and monotonically decreasing with the modulation Σ^2 . On the contrary, with RR $K_{\text{R, coll}}^{(\text{CM})} > 0$ for all η .

III. CV-QKD WITH QAM DISCRETE MODULATION AND PAS

Here we propose a protocol for CV-QKD employing discrete modulation. We start from the scheme in Fig. 1 and we modify only the initial modulation stage, whereas the final detection stage is left unchanged. Alice now draws each couple (x_A, y_A) from the finite set $\mathcal{A} = \Lambda \times \Lambda$, where $\Lambda = \{n\Delta \mid n = -(M-1)/2, \dots, (M-1)/2\}$ contains $M = 2^k$ points, $k \in \mathbb{N}$, and $\Delta \in \mathbb{R}$. Therefore, she has the constellation \mathcal{A} of $M \times M$ symbols depicted in the left panel of Fig. 2, corresponding to a square lattice with pace Δ . This scheme is the so-called quadrature amplitude modulation (QAM) [38], [39]. It is worth noting that in the standard communication notation the points in Λ are commonly placed at distance 2Δ between one another [38], with Δ a scaling factor that determines the mean energy per symbol. Here, for the sake of simplicity, we adopt a different convention by letting such a distance be equal to Δ , which is hence referred to indifferently as scaling factor or symbol spacing.

After the modulation stage, each couple (x_A, y_A) is encoded on its corresponding coherent state $|x_A + iy_A\rangle$, so that the constellation \mathcal{A} is mapped into the (quantum) phase space [47] as a square lattice of $M \times M$ coherent states centred in $(2\sigma_0 x_A, 2\sigma_0 y_A)$ and with pace $2\sigma_0 \Delta$ (right panel of Fig. 2). In the following, we shall discuss the behavior of the present protocol when Alice has the relevant constellations QAM4, QAM16, QAM64, QAM256, associated with the values $M = 2, 4, 8, 16$, respectively.

Remarkably, Alice must generate the values of x_A and y_A by sampling a discrete distribution, and not a continuous one as done in Sec. II. Here we choose the distribution that maximizes the entropy for a given mean energy, namely, the Maxwell–Boltzmann distribution (MB) [27], [40]

$$\mathcal{M}_\beta(z) = \frac{e^{-\beta z^2}}{Z} \quad (z = x_A, y_A) \quad (11)$$

$Z = \sum_z e^{-\beta z^2}$ being the normalization constant.

The considered distribution depends on the two free parameters β (the “inverse temperature”) and Δ (the “spacing factor”) which we shall adjust properly to maximize the performance of the protocol, as discussed in the following subsection. This operation may be implemented in practice through PAS. For the sake of simplicity, in the following we optimize the free parameters to achieve the maximum mutual information between Alice and Bob. Thereafter, we can perform a complete security analysis by discussing all the possible attacks that Eve may launch.

A. Optimization of the Maxwell–Boltzmann distribution

To assign the appropriate values for β and Δ , first of all we introduce a constraint on the constellation energy. This may be achieved by setting the variance of the MB distribution in (11) equal to Σ^2 , namely

$$\text{Var}[z] \equiv \sum_z \mathcal{M}_\beta(z) z^2 = \Sigma^2 \quad (z = x_A, y_A) \quad (12)$$

leading to the overall state

$$\rho_A = \sum_{x_A} \sum_{y_A} \mathcal{M}_\beta(x_A) \mathcal{M}_\beta(y_A) |x_A + iy_A\rangle \langle x_A + iy_A| \quad (13)$$

generated by Alice with mean energy $\bar{n} = 2\Sigma^2$ as in the CM case. Accordingly, also the SNR gets the same value as in the CM case. Indeed, for a given x_A , the conditional probability by Bob in the measurement of the quadrature q reads

$$p_{B|A}(x_B | x_A) = \frac{\exp\left[-(x_B - 2\sigma_0 \sqrt{\eta} x_A)^2 / 2\sigma_0^2\right]}{\sqrt{2\pi\sigma_0^2}} \quad (14)$$

and the corresponding SNR is $\mathbb{E}[x_B]^2 / \text{Var}[x_B] = 4\eta x_A^2$. After averaging over $\mathcal{M}_\beta(x_A)$ we obtain

$$\text{SNR}(\Sigma^2) = 4\eta \Sigma^2. \quad (15)$$

The introduction of the energy constraint induces a dependence between the two free parameters of the MB. In particular, for a given SNR, we exploit (12) to find Δ as a function of β , $\Delta = \Delta(\beta)$ and, in turn, the MB distribution becomes a function of the sole inverse temperature β .

We can search for the optimal value β_{opt} that maximizes the mutual information between Alice and Bob

$$I_{AB}(\beta, \Delta(\beta)) = H_A + H_B - H_{AB} \quad (16)$$

where H_A , H_{AB} , and H_B are the Shannon entropies associated with $p_A(x_A) = \mathcal{M}_\beta(x_A)$, $p_{AB}(x_A, x_B) = \mathcal{M}_\beta(x_A) p_{B|A}(x_B | x_A)$, and $p_B(x_B) = \sum_{x_A} p_{AB}(x_A, x_B)$, respectively.

For simplicity, we consider a fixed channel transmissivity η to highlight the dependency of the SNR on the modulation Σ^2 . This is equivalent to consider a fixed distance between Alice and Bob, provided that the loss rate of optical communication channels is typically around ≈ 0.2 dB/km [48]–[50].

For each Σ^2 (or SNR) we perform the maximization of $I_{AB}(\beta, \Delta(\beta))$ with the golden-section search method [51]. The optimization leads to the optimized parameters β_{opt} and $\Delta_{\text{opt}} = \Delta(\beta_{\text{opt}})$, together with the maximal mutual information

$$I_{AB}^{(\text{opt})} = I_{AB}(\beta_{\text{opt}}, \Delta_{\text{opt}}). \quad (17)$$

The numerical results are shown in the top panel of Fig. 3 for the case $M = 4$ (QAM16) as a function of the modulation variance Σ^2 . The optimal inverse temperature β_{opt} is a decreasing function of Σ^2 . As we can see, for small values of Σ^2 , only the lowest-energy level of the MB in (11) have non-zero probability ($\beta_{\text{opt}} \rightarrow \infty$), so that the optimal constellation tends to a simple QAM4; on the other hand, for large Σ^2 , all the levels of the MB distribution have the same probability $\beta_{\text{opt}} \rightarrow 0$, so that the optimal constellation tends to a uniform QAM16. On the contrary, the spacing Δ_{opt} increases with the modulation:

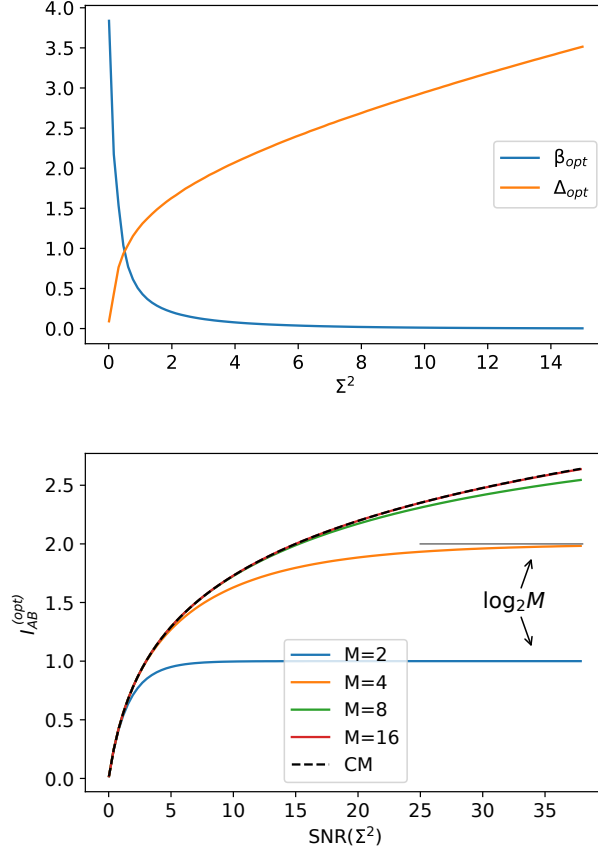


Figure 3. (Top) Optimal inverse temperature β_{opt} and spacing Δ_{opt} as a function of the modulation variance Σ^2 for a QAM16 constellation ($M=4$). (Bottom) Optimized mutual information $I_{AB}^{(opt)}$ as a function of the SNR, where we set $\eta=0.63$ (2 dB attenuation, corresponding to 10 km transmission), and let the SNR vary only with Σ^2 . The dashed line represents the performance of the CM protocol.

the higher the energy, the larger the optimal distance Δ_{opt} between symbols (top panel of Fig. 3). Furthermore, the trend of $I_{AB}^{(opt)}$, plotted in the bottom panel of Fig. 3 as a function of the SNR and for various value of M , shows that there exists a region of small SNR where the QAM modulation formats are effectively able to reach the performance of the CM protocol; the higher M , the larger the region where the QAM format performs optimally. However, for greater SNR values, the sampling distribution becomes more and more uniform and all the curves saturate to the maximum possible entropy of the constellation, namely $\log_2 M$.

B. Security analysis

Now, we are ready to perform the security analysis of the protocol described above. As in Sec. II, we address the cases of individual and collective attacks.

1) *Individual attacks* : For the individual attack case, we consider the particular case where Eve performs homodyne detection of q on her pulse. The performances of alternative detection schemes by Eve are similar.

In the case of DR, the KGR is obtained as

$$K_{D,ind} = I_{AB}^{(opt)} - I_{AE}^{(opt)} \quad (18)$$

where $I_{AE}^{(opt)} = H_A + H_E - H_{AE}$, and the Shannon entropies H_E and H_{AE} are associated with the probability distributions

$$p_{E|A}(x_E | x_A) = \frac{\exp[-(x_E - 2\sigma_0\sqrt{1-\eta}x_A)^2/2\sigma_0^2]}{\sqrt{2\pi\sigma_0^2}} \quad (19)$$

$$p_{AE}(x_A, x_E) = \mathcal{M}_\beta(x_A)p_{E|A}(x_E | x_A) \quad (20)$$

$$p_E(x_E) = \sum_{x_A} p_{AE}(x_A, x_E) \quad (21)$$

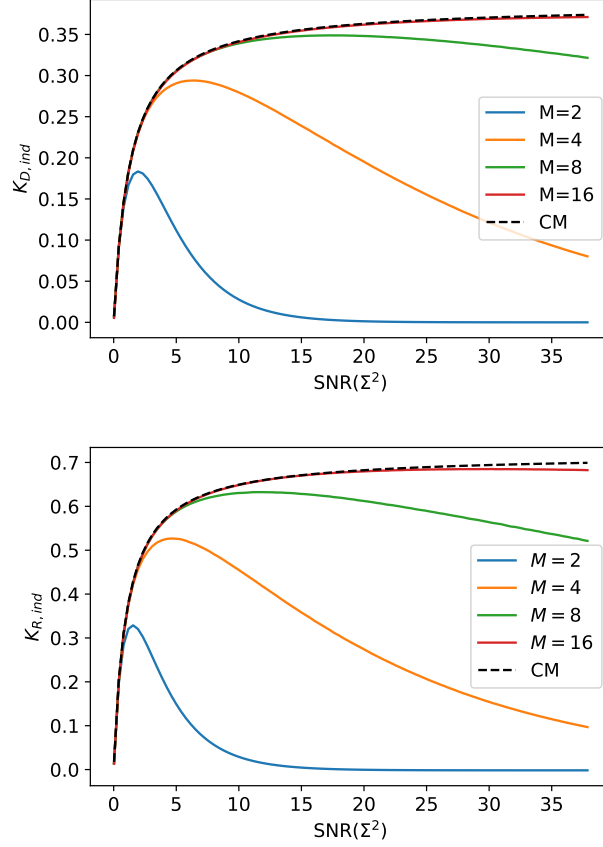


Figure 4. KGR as a function of the SNR for individual attacks and (top panel) DR or (bottom panel) RR. We set $\eta = 0.63$ (2 dB attenuation, i.e., 10 km transmission). The dashed lines represent the performance of the CM protocol.

in which $\mathcal{M}_\beta(x_A)$ is computed with the optimized parameter β_{opt} (and, in turn, Δ_{opt}). In Fig. 4 (top panel) we plot $K_{D,ind}$ as a function of the SNR for a transmissivity $\eta = 0.63$.

In this case, the numerical analysis shows the existence of the threshold transmissivity $\eta = 1/2$, as for the CM case, which can be ascribed to the symmetric role played by Bob and Eve in a DR scenario.

On the contrary, with RR the KGR is

$$K_{R,ind} = I_{AB}^{(opt)} - I_{BE}^{(opt)}. \quad (22)$$

The mutual information $I_{BE}^{(opt)} = H_B + H_E - H_{BE}$ between Bob and Eve can be obtained from the joint probability of Alice, Bob and Eve

$$p_{ABE}(x_A, x_B, x_E) = \frac{\exp[-\beta_{opt} x_A^2]}{Z} \times \frac{\exp[-(x_B - 2\sigma_0 \sqrt{\eta} x_A)^2 / 2\sigma_0^2]}{\sqrt{2\pi\sigma_0^2}} \times \frac{\exp[-(x_E - 2\sigma_0 \sqrt{1-\eta} x_A)^2 / 2\sigma_0^2]}{\sqrt{2\pi\sigma_0^2}}. \quad (23)$$

From the previous equation we can retrieve the joint probability of Bob and Eve $p_{BE}(x_B, x_E) = \sum_{x_A} p_{ABE}(x_A, x_B, x_E)$, the marginal probability of Bob $p_B(x_B) = \int dx_E p_{BE}(x_B, x_E)$, and the marginal probability of Eve $p_E(x_E) = \int dx_B p_{BE}(x_B, x_E)$, together with their associated Shannon entropies. The corresponding $K_{R,ind}$ is depicted in the bottom panel of Fig. 4.

In this case, the numerical results highlight that there is no threshold transmissivity, i.e. $K_{R,ind} > 0$ for all η .

2) *Collective attacks* : If Eve employs a collective attack, the Holevo information should be computed.

With DR, the KGR is obtained as

$$K_{D,coll} = I_{AB}^{(opt)} - \chi_{AE}^{(opt)} \quad (24)$$

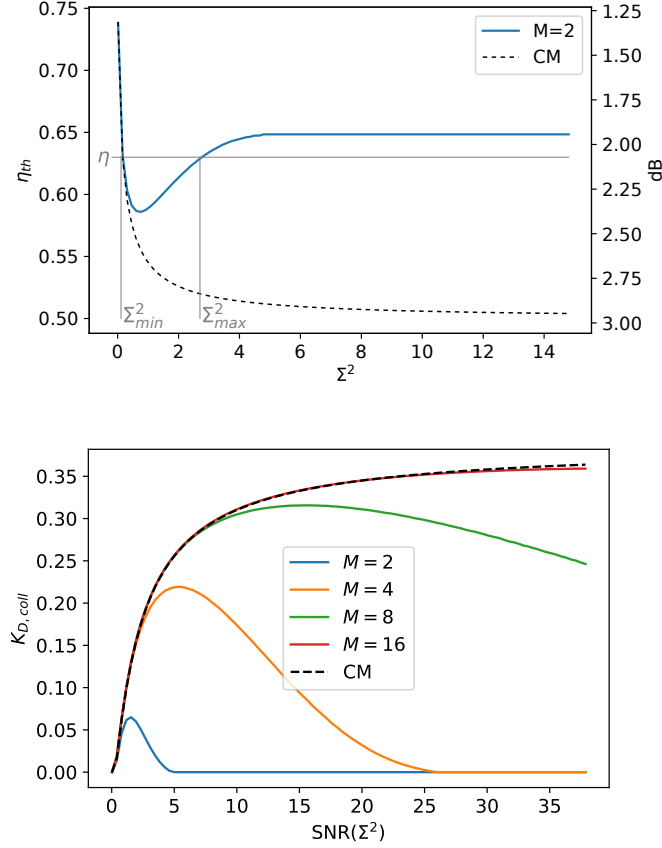


Figure 5. Collective attacks and DR: (Top) threshold transmissivity as a function of the modulation variance. Given η , we identify the regime in which the protocol is successful. (Bottom) KGR as a function of the SNR, where we set $\eta = 0.63$ (2 dB attenuation, i.e., 10 km transmission). The dashed lines represent the performance of the CM protocol.

where $\chi_{AE}^{(\text{opt})} = S[\rho_E] - \sum_{x_A} \mathcal{M}_\beta(x_A) S[\rho_{E|x_A}]$ is the Holevo information between Alice and Eve, with

$$\rho_{E|x_A} = \sum_{y_A} \mathcal{M}_\beta(y_A) |\sqrt{1-\eta}(x_A + iy_A)\rangle \langle \sqrt{1-\eta}(x_A + iy_A)| \quad (25)$$

and

$$\rho_E = \sum_{x_A} \mathcal{M}_\beta(x_A) \rho_{E|x_A}. \quad (26)$$

As we did above, in all the previous expressions the MB distribution is computed with the optimized parameters. The Holevo information $\chi_{AE}^{(\text{opt})}$ has to be evaluated numerically through direct diagonalization of ρ_E and $\rho_{E|x_A}$.

The numerical results show that $K_{D,\text{coll}} > 0$ for $\eta > \eta_{\text{th}}(\Sigma^2)$ as in the CM case. However, now the function $\eta_{\text{th}}(\Sigma^2)$ is not monotonic: it has a minimum η_{min} and then saturates to an asymptotic value η_∞ , as shown in the top panel of Fig. 5 for the QAM4 case. Therefore, given the transmissivity η , three scenarios are possible:

- 1) $\eta \leq \eta_{\text{min}}$: the protocol does not work and we have $K_{D,\text{coll}} = 0$;
- 2) $\eta_{\text{min}} < \eta < \eta_\infty$: there exist a lower and an upper threshold, $\Sigma_{\text{min}}^2(\eta)$ and $\Sigma_{\text{max}}^2(\eta)$, respectively, and the protocol is successful only in the regime $\Sigma_{\text{min}}^2(\eta) \leq \Sigma^2 \leq \Sigma_{\text{max}}^2(\eta)$;
- 3) $\eta_\infty \leq \eta \leq 1$: there exists only the lower threshold $\Sigma_{\text{min}}^2(\eta)$, while $\Sigma_{\text{max}}^2(\eta) = \infty$.

The KGR with collective attacks and DR is plotted in the bottom panel of Fig. 5 as a function of the SNR.

If we consider RR, the KGR is

$$K_{R,\text{coll}} = I_{AB}^{(\text{opt})} - \chi_{BE}^{(\text{opt})} \quad (27)$$

where $\chi_{BE}^{(\text{opt})} = S[\rho_E] - \int dx_B p_B(x_B) S[\rho_{E|x_B}]$ is the Holevo information between Bob and Eve; ρ_E the density matrix in (26); $p_B(x_B) = \sum_{x_A} \mathcal{M}_\beta(x_A) p_{B|A}(x_B|x_A)$; and $p_{B|A}(x_B|x_A)$ as in (14). To calculate the conditional state $\rho_{E|x_B}$ we consider the joint state of Bob and Eve, $\rho_{BE} = U_{BS}(\eta) \rho_A \otimes |0\rangle\langle 0| U_{BS}(\eta)^\dagger$, with ρ_A given in (13) and U_{BS} is the operator associated with

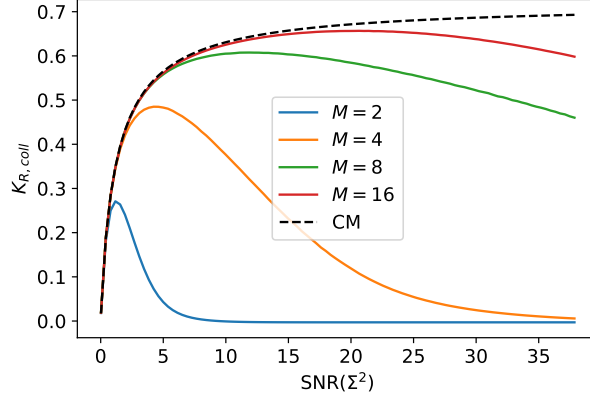


Figure 6. KGR as a function of the SNR for collective attacks and RR. We set $\eta = 0.63$ (2 dB attenuation, i.e., 10 km transmission). The dashed lines represent the performances of the CM protocol.

the beam splitter with transmissivity η [13] depicted in Fig. 1. After straightforward calculation we get

$$\rho_{BE} = \sum_{x_A, y_A} \mathcal{M}_\beta(x_A) \mathcal{M}_\beta(y_A) \times |\sqrt{\eta}(x_A + iy_A)\rangle \langle \sqrt{\eta}(x_A + iy_A)| \otimes |\sqrt{1-\eta}(x_A + iy_A)\rangle \langle \sqrt{1-\eta}(x_A + iy_A)|. \quad (28)$$

After Bob's measurement, given the outcome x_B , Eve's conditional state writes [47]

$$\rho_{E|x_B} = \frac{1}{p_B(x_B)} \sum_{x_A, y_A} p_{AB}(x_A, x_B) \mathcal{M}_\beta(y_A) |\sqrt{1-\eta}(x_A + iy_A)\rangle \langle \sqrt{1-\eta}(x_A + iy_A)|. \quad (29)$$

Again, calculations require a numerical diagonalization of ρ_E and $\rho_{E|x_B}$. The resulting $K_{R, \text{coll}}$, plotted in Fig. 6, does not show any threshold transmissivity, that is $K_{R, \text{coll}} > 0, \forall \eta$ and $\forall M$.

The results of Fig. 4, 5, and 6 lead to the same qualitative behavior. For small SNR, a discrete alphabet is able to retrace the results of the CM protocol, attaining the same KGR. However, in contrast with the CM case, the KGR increases with the SNR only up to a maximum, after which it decreases again and approaches 0. This is due to the finite size of the constellation, which causes both the mutual information and the Holevo information to saturate to a finite value. Indeed, since the number of symbols is fixed, increasing the SNR (i.e., increasing the mean number of photons per symbol $\bar{n} = 2\Sigma^2$) induces an increase in the spacing Δ between symbols, as shown in Fig. 3, making them more “distinguishable”. On the contrary, if the SNR is small enough, the encoded symbols are hidden behind the shot noise, guaranteeing a higher security of the protocol.

Remarkably, even with nearly distinguishable pulses, our results show that in the case of RR Eve cannot gain more information than Bob, keeping the protocol secure for any Σ^2 . Yet, for a given modulation order, there is an optimal SNR that maximizes the KGR, and a limited SNR range in which the protocol yields a practically relevant KGR.

Moreover, once fixed a working range for the SNR, it is always possible to find a finite $M \times M$ QAM alphabet, with sufficiently large M and optimized MB distribution, to approach with arbitrary accuracy the KGR achieved by the CM protocol.

IV. A MORE SOPHISTICATED OPTIMIZATION PROCEDURE

In the previous section we have proceeded by choosing the optimal values β_{opt} and Δ_{opt} that maximize the mutual information between Alice and Bob.

However, given the previous discussion, a feasible alternative emerges, in which the values of the free parameters are selected to maximize directly the KGR, instead of the sole mutual information $I_{AB}(\beta, \Delta(\beta))$. As in the strategy of Sec. III-A, the spacing $\Delta(\beta)$ is obtained as a function of the inverse temperature β thanks to the energy constraint of (12); however, differently from that strategy, the optimal inverse temperature is obtained as

$$\beta_{\text{opt}} = \arg \max_{\beta} \text{KGR} \quad (30)$$

with the expressions of the KGR defined in (18), (22), (24), or (27), according to the case in exam.

Such a task is straightforward but not trivial to implement, especially for collective attacks. Indeed, if we wanted to implement a golden-section-search method as in Sec. III-A, in any step of the numerical algorithm we should compute not only $I_{AB}(\beta, \Delta(\beta))$ but also the density matrices ρ_E and $\rho_{E|x_A/x_B}$, with a much higher computational cost. Here, for simplicity, we discuss only the simplest case concerning the individual attacks with DR. The analysis of the other scenarios will be performed elsewhere.

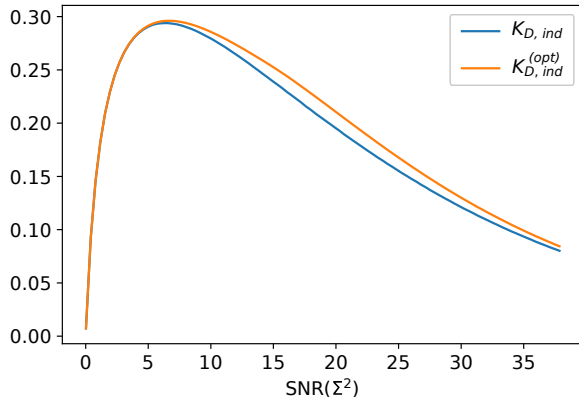


Figure 7. KGR as a function of the SNR for individual attacks and DR, considering either a suboptimal or optimal MB distribution. We set $\eta = 0.63$ (2 dB attenuation, i.e., 10 km transmission).

Now we have $\beta_{\text{opt}} = \arg \max_{\beta} K_{D, \text{ind}}(\beta, \Delta(\beta))$, $\Delta_{\text{opt}} = \Delta(\beta_{\text{opt}})$, and the optimized

$$K_{D, \text{ind}}^{(\text{opt})} = K_{D, \text{ind}}(\beta_{\text{opt}}, \Delta_{\text{opt}}). \quad (31)$$

The corresponding results are reported in Fig. 7. For small SNR, the optimization procedure is equivalent to that of Sec. III-A and both strategies allow to reach the maximum performance of the channel. Otherwise, for larger Σ^2 , optimizing $K_{D, \text{ind}}$ makes the protocol more robust, leading to a higher KGR. At the same time, these results prove themselves as a validation for the mutual information optimization method, which is fully optimal for small SNR and sub-optimal for larger SNR.

V. CONCLUSION

In this paper we have proposed a CV-QKD protocol employing the discrete modulation formats typically exploited in classical telecommunications. We have embedded the QAM format into the GG02 protocol originally proposed in [6] and exploited PAS to increase the amount of security for a given modulation level. In our proposal, the sender has only a finite set of coherent pulses available, constituting a square constellation of $M \times M$ states, generated by sampling a Maxwell-Boltzmann distribution. The receiver performs a homodyne measurement of q/p , chosen at random, on his received signal. Then we have evaluated the optimized sender probability distribution to maximize the shared mutual information. The security analysis has shown that our discrete modulation protocol reaches the capacity of the channel in appropriate regimes of SNR. Finally, we have proposed a better optimization strategy, based on the direct maximization of the KGR instead of the sole mutual information. We have discussed the case of individual attacks with direct reconciliation and we have proved the method to be more powerful.

Our results prove that a suitable PAS of a discrete constellation allows to overcome the finite transmitter dynamics and to approximate the performance of the standard CV-QKD based on CM also for increasing average powers. Moreover, they pave the way for the design of feasible schemes compatible with the currently exploited telecom techniques.

REFERENCES

- [1] R. L. Rivest, A. Shamir, and L. Adleman, "A method for obtaining digital signatures and public-key cryptosystems," *Commun. ACM*, vol. 21, no. 2, pp. 120–126, 1978.
- [2] G. S. Vernam, "Cipher printing telegraph systems for secret wire and radio telegraphic communications," *Trans. AIEE*, vol. XLV, pp. 295–301, 1926.
- [3] C. E. Shannon, "Communication theory of secrecy systems," *Bell Syst. Tech. J.*, vol. 28, no. 4, pp. 656–715, 1949.
- [4] C. H. Bennett and G. Brassard, "Quantum cryptography: Public-key distribution and coin tossing," in *Proc. IEEE Int. Conf. on Computers, Systems and Signal Processing*, Bangalore, India, 1984, pp. 175–179.
- [5] A. K. Ekert, "Quantum cryptography and Bell's theorem," in *Quantum Measurements in Optics*. Springer, 1992, pp. 413–418.
- [6] F. Grosshans and P. Grangier, "Continuous variable quantum cryptography using coherent states," *Phys. Rev. Lett.*, vol. 88, Art. no. 057902, Jan 2002.
- [7] N. Gisin, G. Ribordy, W. Tittel, and H. Zbinden, "Quantum cryptography," *Rev. Mod. Phys.*, vol. 74, pp. 145–195, Mar 2002.
- [8] W. K. Wootters and W. H. Zurek, "A single quantum cannot be cloned," *Nature*, vol. 299, no. 5886, pp. 802–803, 1982.
- [9] T. C. Ralph, "Continuous variable quantum cryptography," *Phys. Rev. A*, vol. 61, Art. no. 010303, Dec 1999.
- [10] F. Grosshans *et al.*, "Quantum key distribution using Gaussian-modulated coherent states," *Nature*, vol. 421, no. 6920, pp. 238–241, 2003.
- [11] F. Grosshans, A. Acín, and N. Cerf, "Continuous-variable quantum key distribution," in *Quantum information with continuous variables of atoms and light*. World Scientific, 2007, pp. 63–83.
- [12] E. Diamanti and A. Leverrier, "Distributing secret keys with quantum continuous variables: Principle, security and implementations," *Entropy*, vol. 17, no. 9, pp. 6072–6092, 2015.

- [13] S. Olivares, “Introduction to generation, manipulation and characterization of optical quantum states,” *Phys. Lett. A*, vol. 418, Art. no. 127720, Dec 2021.
- [14] J. Lodewyck, T. Debuisschert, R. Tualle-Brouiri, and P. Grangier, “Controlling excess noise in fiber-optics continuous-variable quantum key distribution,” *Phys. Rev. A*, vol. 72, Art. no. 050303, Nov 2005.
- [15] J. Lodewyck *et al.*, “Quantum key distribution over 25 km with an all-fiber continuous-variable system,” *Phys. Rev. A*, vol. 76, Art. no. 042305, Oct 2007.
- [16] S. Fossier *et al.*, “Field test of a continuous-variable quantum key distribution prototype,” *New J. Phys.*, vol. 11, no. 4, Art. no. 045023, Apr 2009.
- [17] M. Hillery, “Quantum cryptography with squeezed states,” *Phys. Rev. A*, vol. 61, Art. no. 022309, Jan 2000.
- [18] M. D. Reid, “Quantum cryptography with a predetermined key, using continuous-variable Einstein-Podolsky-Rosen correlations,” *Phys. Rev. A*, vol. 62, Art. no. 062308, Nov 2000.
- [19] C. E. Shannon, “A mathematical theory of communication,” *Bell Syst. Tech. J.*, vol. 27, no. 3/4, pp. 379–423/623–656, July/Oct 1948.
- [20] R. G. Gallager, *Information Theory and Reliable Communication*. New York: Wiley, 1968.
- [21] G. Böcherer, F. Steiner, and P. Schulte, “Bandwidth efficient and rate-matched low-density parity-check coded modulation,” *IEEE Trans. Commun.*, vol. 63, no. 12, pp. 4651–4665, 2015.
- [22] F. Buchali *et al.*, “Rate adaptation and reach increase by probabilistically shaped 64-QAM: An experimental demonstration,” *J. Light. Technol.*, vol. 34, no. 7, pp. 1599–1609, 2016.
- [23] T. Fehenberger, A. Alvarado, G. Böcherer, and N. Hanik, “On probabilistic shaping of quadrature amplitude modulation for the nonlinear fiber channel,” *J. Light. Technol.*, vol. 34, no. 21, pp. 5063–5073, 2016.
- [24] P. Schulte and G. Böcherer, “Constant composition distribution matching,” *IEEE Trans. Inf. Theory*, vol. 62, no. 1, pp. 430–434, 2015.
- [25] S. Civelli and M. Secondini, “Hierarchical distribution matching for probabilistic amplitude shaping,” *Entropy*, vol. 22, no. 9, Art. no. 958, 2020.
- [26] Y. C. Gültekin, T. Fehenberger, A. Alvarado, and F. M. Willems, “Probabilistic shaping for finite blocklengths: Distribution matching and sphere shaping,” *Entropy*, vol. 22, no. 5, Art. no. 581, 2020.
- [27] F. R. Kschischang and S. Pasupathy, “Optimal nonuniform signaling for Gaussian channels,” *IEEE Trans. Inf. Theory*, vol. 39, no. 3, pp. 913–929, 1993.
- [28] F. Buchali *et al.*, “Experimental demonstration of capacity increase and rate-adaptation by probabilistically shaped 64-QAM,” in *2015 European Conference on Optical Communication (ECOC)*. IEEE, 2015, pp. 1–3.
- [29] T. Fehenberger *et al.*, “Sensitivity gains by mismatched probabilistic shaping for optical communication systems,” *IEEE Photon. Technol. Lett.*, vol. 28, no. 7, pp. 786–789, 2016.
- [30] A. Leverrier and P. Grangier, “Unconditional security proof of long-distance continuous-variable quantum key distribution with discrete modulation,” *Phys. Rev. Lett.*, vol. 102, Art. no. 180504, May 2009.
- [31] A. Leverrier and P. Grangier, “Continuous-variable quantum key distribution protocols with a discrete modulation,” arXiv:1002.4083 [quant-ph], 2010.
- [32] A. Leverrier and P. Grangier, “Continuous-variable quantum-key-distribution protocols with a non-Gaussian modulation,” *Phys. Rev. A*, vol. 83, Art. no. 042312, Apr 2011.
- [33] A. Becir, F. A. A. El-Orany, and M. R. B. Wahiddin, “Continuous-variable quantum key distribution protocols with eight-state discrete modulation,” *Int. J. Quantum Inf.*, vol. 10, no. 01, Art. no. 1250004, 2012.
- [34] T. Hirano *et al.*, “Implementation of continuous-variable quantum key distribution with discrete modulation,” *Quantum Sci. Technol.*, vol. 2, no. 2, Art. no. 024010, 2017.
- [35] S. Ghorai, P. Grangier, E. Diamanti, and A. Leverrier, “Asymptotic security of continuous-variable quantum key distribution with a discrete modulation,” *Phys. Rev. X*, vol. 9, Art. no. 021059, Jun 2019.
- [36] J. Lin, T. Upadhyaya, and N. Lütkenhaus, “Asymptotic security analysis of discrete-modulated continuous-variable quantum key distribution,” *Phys. Rev. X*, vol. 9, Art. no. 041064, Dec 2019.
- [37] A. Denys, P. Brown, and A. Leverrier, “Explicit asymptotic secret key rate of continuous-variable quantum key distribution with an arbitrary modulation,” *Quantum*, vol. 5, Art. no. 540, Sep. 2021.
- [38] J. G. Proakis, *Digital Communications*, 4th ed. McGraw Hill, 2001.
- [39] G. Cariolaro, *Quantum communications*. Springer, 2015.
- [40] T. M. Cover and J. A. Thomas, *Elements of Information Theory*, 2nd ed. Hoboken, NJ: Wiley, 2006.
- [41] H. Taub and D. L. Schilling, *Principles of communication systems*. McGraw-Hill Higher Education, 1986.
- [42] G. D’Ariano, C. Macchiavello, and M. G. A. Paris, “Information gain in quantum communication channels,” in *Quantum Communications and Measurement*. Springer, 1995, pp. 339–350.
- [43] G. Van Assche, J. Cardinal, and N. J. Cerf, “Reconciliation of a quantum-distributed Gaussian key,” *IEEE Trans. Inf. Theory*, vol. 50, no. 2, pp. 394–400, 2004.
- [44] C. H. Bennett, G. Brassard, C. Crépeau, and U. M. Maurer, “Generalized privacy amplification,” *IEEE Trans. Inf. Theory*, vol. 41, no. 6, pp. 1915–1923, 1995.
- [45] A. S. Holevo, “The capacity of the quantum channel with general signal states,” *IEEE Trans. Inf. Theory*, vol. 44, no. 1, pp. 269–273, 1998.
- [46] F. Grosshans, “Collective attacks and unconditional security in continuous variable quantum key distribution,” *Phys. Rev. Lett.*, vol. 94, Art. no. 020504, Jan 2005.
- [47] S. Olivares, “Quantum optics in the phase space,” *Eur. Phys. J. Spec. Top.*, vol. 203, no. 1, pp. 3–24, Apr 2012.
- [48] G. P. Agrawal, *Fiber-optic communications systems*, 3rd ed. Wiley, 2002.

- [49] P. Jouguet *et al.*, “Experimental demonstration of long-distance continuous-variable quantum key distribution,” *Nat. Photonics*, vol. 7, no. 5, pp. 378–381, May 2013.
- [50] J. Lodewyck, T. Debuisschert, R. Tualle-Brouri, and P. Grangier, “Controlling excess noise in fiber-optics continuous-variable quantum key distribution,” *Phys. Rev. A*, vol. 72, no. 5, Art. no. 050303, Nov 2005.
- [51] W. H. Press, S. A. Teukolsky, W. T. Vetterling, and B. P. Flannery, *Numerical recipes 3rd edition: The art of scientific computing*. Cambridge University Press, 2007.